J Solid State Electrochem (2009) 13:1535–1539
DOI 10.1007/s10008-008-0723-z

ORIGINAL PAPER

Electrochemical behavior and stability of $Li_4Ti_5O_{12}$ in a broad voltage window

Jie Shu

Received: 23 August 2008 / Revised: 13 October 2008 / Accepted: 27 October 2008 / Published online: 11 November 2008

Abstract Electrochemical behavior and stability of spinel $Li_4Ti_5O_{12}$ are investigated in a broad voltage window (0.0–5.0 V vs. Li/Li^+). The voltage profile of the $Li_4Ti_5O_{12}$ electrode shows a plateau region at 1.55 V and two sloped regions below 1.55 V when the electrode is cycled between 0.0 and 2.0 V. It is found that $Li_4Ti_5O_{12}$ maintains high lithium storage characteristic with the increase of the current density. Moreover, $Li_4Ti_5O_{12}$ shows excellent rate performance in 0.0–2.0 V and good cyclic performances in 0.0–4.0 and 1.0–5.0 V. Besides, the crystal structure is kept when it is cycled between 0.0 and 5.0 V.

Keywords $Li_4Ti_5O_{12}$ · Broad electrochemical window · Lithium ion batteries

Introduction

$Li_4Ti_5O_{12}$ attracts much attention as anode material for lithium ion batteries and asymmetric supercapacitor due to its excellent cyclic performance [1–3]. This is mainly related to its negligible structure variation during lithium insertion/extraction. It was reported that the variation of the lattice parameter is confined between 0.1% and 0.3%, when it is cycled in the voltage range from 1.0 to 2.0 V [4–6]. In addition, the surface of particles is free of solid electrolyte interphase (SEI) film in this voltage range [7].

$Li_4Ti_5O_{12}$ has a face-centered cubic spinel structure (F_{d3m}) where the tetrahedral 8a sites are fully taken up by lithium and the octahedral 16d sites are randomly occupied by lithium and titanium with an atomic ratio of 1:5 in a cubic close-packed oxygen array. $Li_4Ti_5O_{12}$ can be described as $[Li]_{8a}[Ti_{5/3}Li_{1/3}]_{16d}[O_4]_{32e}$. Octahedral 16c sites and tetrahedral 8b and 48f sites are empty. Upon the insertion of three lithium ions, three lithium atoms at 8a sites will transfer to 16c sites, and the inserted three lithium ions also occupy 16c sites via 8a sites. Finally, it transforms into $Li_7Ti_5O_{12}$ ($[Li_2]_{16c}[Ti_{5/3}Li_{1/3}]_{16d}[O_4]_{32e}$), and three Ti^{4+} ions are reduced to Ti^{3+} ions. This process is corresponding to a voltage plateau at 1.55 V in the voltage profile. The theoretical specific capacity is 175 mAh g^{-1}, and the practical reversible capacity is about 160 mAh g^{-1} [8, 9]. However, $Li_4Ti_5O_{12}$ can deliver a theoretical capacity of 296 mAh g^{-1} according to the reduction of all Ti^{4+} in the compound. Besides, some cathode materials (such as $LiCoO_2$ and $LiMn_2O_4$) were modified by $Li_4Ti_5O_{12}$ [10, 11]. Therefore, it is important to get a clear understanding of the Li-insertion/extraction behaviors of $Li_4Ti_5O_{12}$ in a broader electrochemical window (0.0–5.0 V) and know its electrochemical performance and stability.

Experimental

Spinel $Li_4Ti_5O_{12}$ powder was synthesized through a solid state reaction using TiO_2-anatase (99.9 %) and Li_2CO_3 (99.99 %) as starting materials. The precursors were ball-milled for 8 h and calcined at 850 °C for 24 h in air, then cooled down to room temperature naturally.

The electrode was prepared by pasting a slurry containing 82 wt.% $Li_4Ti_5O_{12}$, 10 wt.% carbon black (CB), and 8 wt.% polyvinylidene fluoride (PVDF) dissolved in *N*-methylpyrolline onto a copper foil or titanium foil. Ti foil

J. Shu (✉)
Institute of Physics, Chinese Academy of Sciences,
Beijing 100190, People's Republic of China
e-mail: sjshujie@126.com

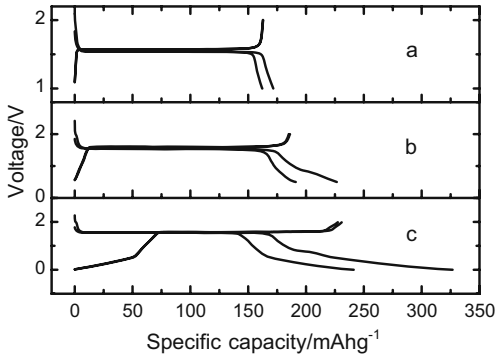

Fig. 1 The first and second charge–discharge curves of $Li_4Ti_5O_{12}$ achieved at a current density of 0.078 mA cm^{-2} in different voltage ranges. **a** 1.0–2.0 V; **b** 0.5–2.0 V; **c** 0.0–2.0 V

was used as current collector when the charging voltage is beyond 3.5 V. After coating, the film was dried in a vacuum oven at 100 °C for 12 h and pressed and cut into a sheet with an area of 0.64 cm^2. Before using, the sheet was dried in a vacuum chamber at 120 °C for 12 h. A two-electrode cell was constructed in an argon-filled glove box using a metal lithium foil as counter electrode, 1 M $LiPF_6$ dissolved in a 1:1 *v*/*v* mixture of ethylene carbonate (EC) and dimethyl carbonate (DMC) as electrolyte and Celgard® 2300 as separator.

X-ray diffraction (XRD) patterns were collected using a Rigaku B/max-2400 X-ray diffractometer with CuKα radiation. The morphologies of electrodes were investigated with a Hitachi S-4000 scanning electron microscopy (SEM). Galvanostatic charge/discharge cycling was tested on a Land Battery Test System. All the electrochemical tests were carried out at 25 °C.

Result and discussions

The powder X-ray diffraction pattern of the obtained material demonstrates that it is pure $Li_4Ti_5O_{12}$, and the average size of particles is 0.3–0.8 μm as observed by SEM. They are primary crystallites. The voltage curves in different cycling ranges are shown in Fig. 1. The voltage profile for the electrode cycled between 1.0 and 2.0 V is similar with those reported in [4–6]. It is obvious that the reaction of $Li_4Ti_5O_{12}$ with lithium ion shows one typical reversible insertion/extraction process when the amount of inserted lithium ions are limited within three. The electrochemical reaction of $Li_4Ti_5O_{12}$ toward lithium ion can be described as the following:

$$[Li]_{8a}[]_{16c}\left[Ti_{5/3}Li_{1/3}\right]_{16d}[O_4]_{32e}+Li^+ + e^- \rightleftarrows []_{8a}[Li_2]_{16c}\left[Ti_{5/3}Li_{1/3}\right]_{16d}[O_4]_{32e} \quad (1)$$

The subscripts outside the bracket in Eq. 1 show the lattice sites. As mentioned above, lithium atoms at 8a sites move to 16c sites and the inserted lithium ions also occupy 16c sites via 8a site in the discharge process. During extraction, lithium atoms are extracted out from 16c sites via 8a sites, and the other lithium atoms move back to 8a sites from 16c sites. Obviously, this process is highly reversible and should be energy favorable. This mechanism has been clearly confirmed by Ohzuku et al. [8]. In the case of the electrode discharged to 0.5 V, the charge curve is mainly composed of two regions, including a slope below 1.55 V (12 mAh g^{-1}) and a plateau at 1.55 V (159 mAh g^{-1}). In the case of the electrode discharged to 0.0 V, the charge–discharge curves are mainly composed of three regions, including two slopes below 1.55 V (70 mAh g^{-1}) and a plateau at 1.55 V (155 mAh g^{-1}). The appearance of the sloped regions indicates the new electrochemical insertion processes below 1.55 V.

It is noticed from Fig. 1 that there is an irreversible capacity loss when the cutoff voltage for discharging is limited below 1.0 V. This is supposed to be caused mainly by the formation of a solid electrolyte interphase film on the surface of $Li_4Ti_5O_{12}$ particles [12]. As evidenced upon cycling, the SEI film is stable in 0.0–3.0 V. Therefore, the appearance of the sloped regions in Fig. 1 clearly indicates that there is a different lithium insertion/extraction mechanism, compared with the plateau region at 1.55 V, which is related to the uptake/release of lithium at 16 c sites. Cyclic performances of $Li_4Ti_5O_{12}$ are shown in Fig. 2. It can be seen that the capacity retention is still quite good even if the electrode was cycled between 0.0 and 2.0 V.

When more than three lithium ions per formula were inserted as shown in Fig. 1, 8a,8b, and 48f sites could be occupied further since 16c sites are fully occupied already.

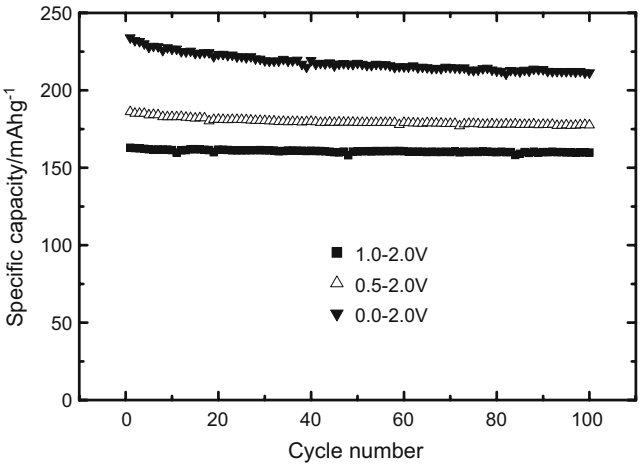

Fig. 2 Specific capacity vs. cycle number profiles of $Li_4Ti_5O_{12}$ cycled at a current density of 0.078 mA cm^{-2} in the range of 1.0–2.0, 0.5–2.0, 0.0–2.0 V, respectively

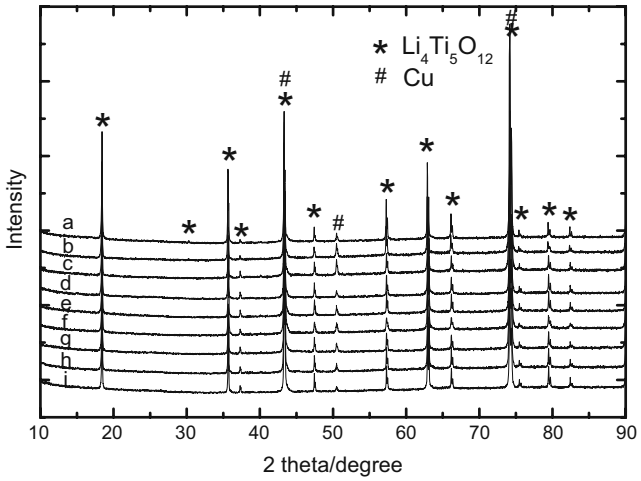

Fig. 3 Ex situ XRD patterns of $Li_4Ti_5O_{12}$ cycled between 0.0 and 2.0 V. **a** Discharged to 2.0 V, **b** discharged to 1.55 V, **c** discharged to 0.8 V, **d** discharged to 0.5 V, **e** discharged to 0.3 V, **f** discharged to 0.0 V, **g** charged to 0.3 V, **h** charged to 0.5 V, **i** charged to 2.0 V

The occupation of lithium at these sites cannot change the spinel structure. The environment for 8a and 8b sites is equivalent. Therefore, the insertion/extraction should not be interfered if 8a sites or 8b sites besides 16c sites are occupied during lithium insertion. It was reported that $Li_4Ti_5O_{12}$ can be lithiated chemically, and some lithium ions occupy 48f sites but cannot be extracted out electrochemically [13]. Thus, the occupation of 48f sites may be the cause of capacity fading during cycling between 0.0 and 3.0 V.

In order to determine the lithiation mechanism of $Li_4Ti_5O_{12}$ at highly lithiated states, ex situ XRD patterns of $Li_4Ti_5O_{12}$ cycled in 0.0–2.0 V are recorded in Fig. 3. It is found that no phase transition and amorphous phase are observed during cycling. Figure 4 shows the variation of the lattice parameter. It decreases with the insertion of lithium and restores after lithium extraction. According to the calculation of lattice parameter, it is clear that the whole volume change is less than 0.1% during cycling in this voltage range. Therefore, it indicates that the increased reversible capacity in 0–1.55 V for $Li_4Ti_5O_{12}$ is related to

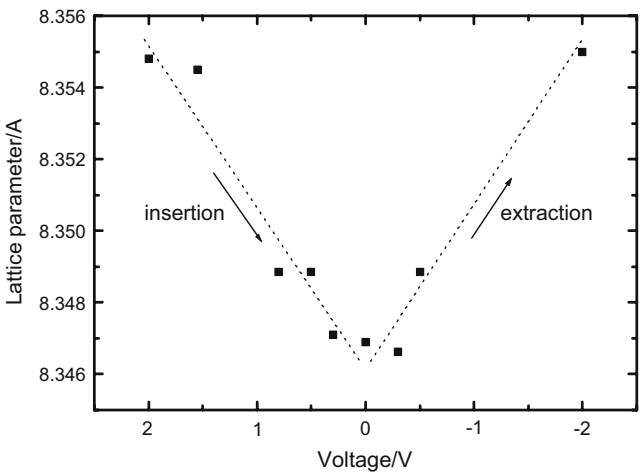

Fig. 4 Lattice parameter evolution of $Li_4Ti_5O_{12}$ during the first galvanostatic cycling between 0.0 and 2.0 V

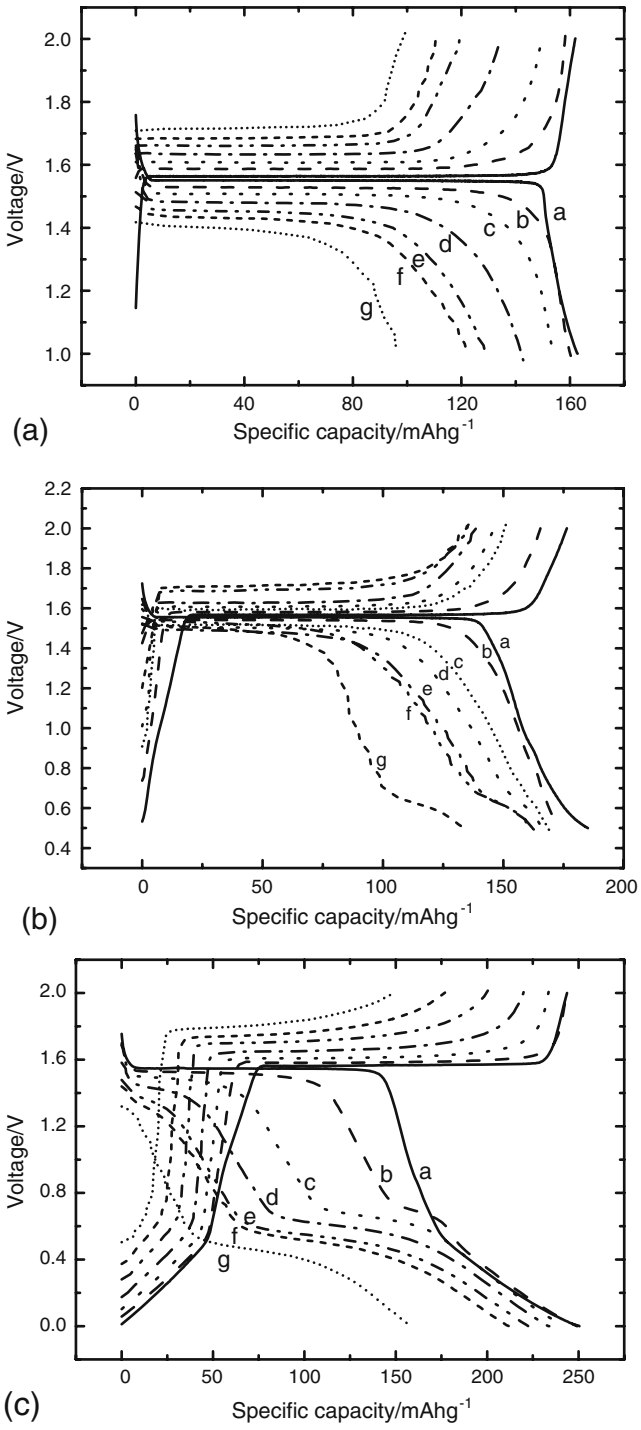

Fig. 5 Charge and discharge curves of $Li_4Ti_5O_{12}$ obtained at different rates in different voltage ranges of 1.0–2.0, 0.5–2.0, and 0.0–2.0. **a** 0.078 mA cm^{-2}, **b** 0.78 mA cm^{-2}, **c** 1.56 mA cm^{-2}, **d** 3.12 mA cm^{-2}, **e** 4.68 mA cm^{-2}, **f** 6.24 mA cm^{-2}, **g** 7.8 mA cm^{-2}

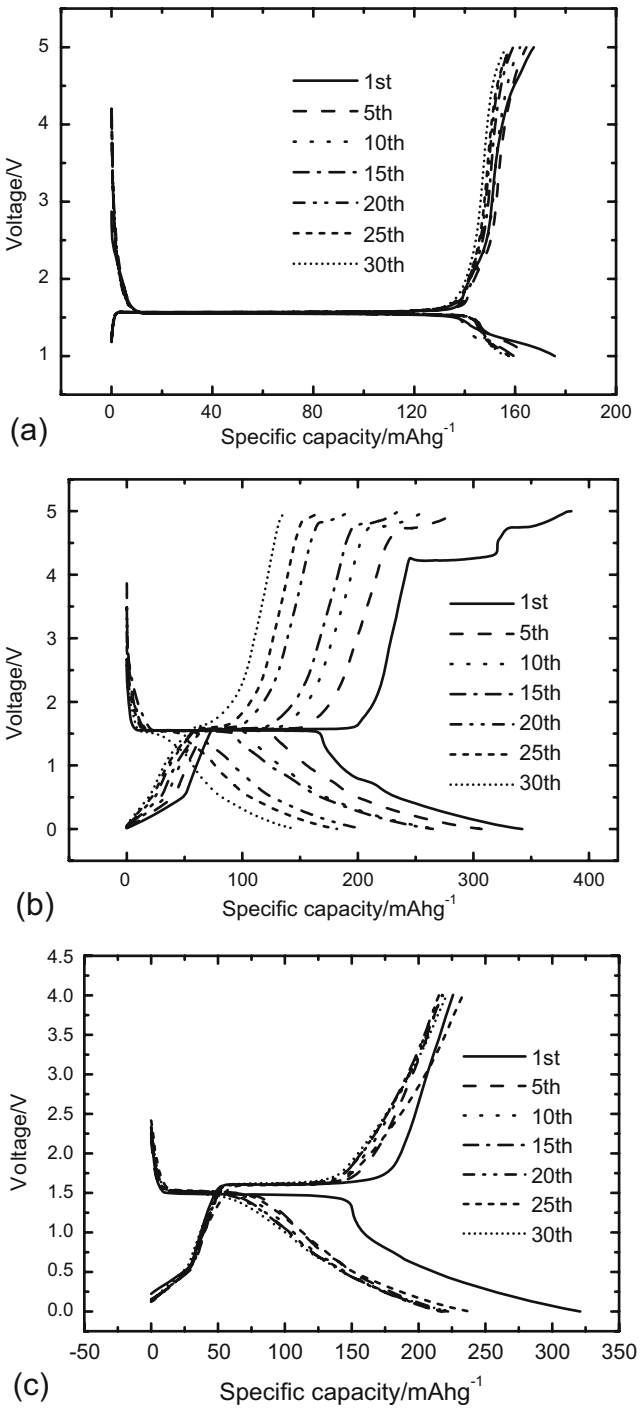

Fig. 6 Charge and discharge profiles of $Li_4Ti_5O_{12}$ cycled at a current density of 0.078 mA cm^{-2} in different voltage ranges of **a** 1.0–5.0, **b** 0.0–5.0, and **c** 0.0–4.0 V

certain reversible intercalation processes instead of a reduction–decomposition reaction as reported in other transition metal oxides or an interfacial charging process in nanocomposite [14–18]. As shown in Figs. 1 and 2, there are two slopes from 1.55 to 0.0 V. This means that lithium ions should occupy two types of sites with different energies, besides 16c sites. As mentioned above, it could be tetrahedral 8a, 8b, or 48f sites.

The rate performance of $Li_4Ti_5O_{12}$ in the narrow voltage range from 1.0 to 2.0 V is shown in Fig. 5a. This result is similar with the studies by others. The capacity decreases from 155 mAh g^{-1} at 0.078 mA cm^{-2} (0.1 °C) to 100 mAh g^{-1} at 7.8 mA cm^{-2} (10 °C), indicating an excellent rate performance. It can be seen that the voltage profiles are not influenced by the current densities. However, it is surprising to observe that the voltage profiles for Li insertion are influenced strongly by the current density when the voltage limitation is below 1.0 V (see Fig. 5b,c). The capacity for the plateau at 1.55 V decreases, and a new plateau appears at 0.5–0.6 V with the increase of discharge current density. Furthermore, the corresponding capacity enhances with the current density increase from 0.078 to 7.8 mA cm^{-2}. However, the sum of the capacities for these two plateaus does not change too much at different current densities. Viewed from Fig. 5, the voltage profiles for charging are not influenced strongly by the current density. Superior rate properties are also presented in this broad electrochemical window. Even though the current density as high as 7.8 mA cm^{-2} is given, a reversible specific capacity of 150 mAh g^{-1} can be delivered when the material was cycled between 0.0 and 2.0 V. To this cycling range, about 80% capacity of the maximum reversible capacity can still be maintained when the current density was increased from 0.078 to 7.8 mA cm^{-2}.

The stability of $Li_4Ti_5O_{12}$ in a broader electrochemical window is investigated as shown in Figs. 6 and 7. Excellent cycle life is demonstrated when the battery was cycled between 1.0 and 5.0 V, which is comparable to that obtained in 1.0–2.0 V. No extra electrochemical reactions are observed. This means that lithium cannot be extracted out from 8a sites and 16d sites in spinel $Li_4Ti_5O_{12}$. This is also supported by the fact that no electrochemical response is

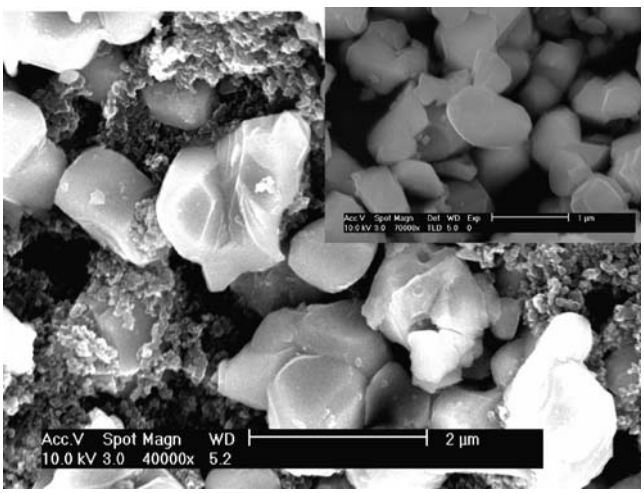

Fig. 7 SEM image of $Li_4Ti_5O_{12}$ cycled in the voltage range 1.0–5.0 V. Sample before cycling is shown in the *inline image*

observed when the electrode was cycled in the voltage range 2.0–5.0 V. In case that the electrode was cycled between 0.0 and 5.0 V, an unusual voltage profile is observed above 4.2 V (Fig. 6b), which part is irreversible. However, the extra oxidation reactions are not observed when the electrode was cycled between 0.0 and 4.0 V. As we mentioned above, the SEI film was formed when the electrode was discharged below 1.0 V. Comparing Fig. 6a,b with c, it suggests that the unusual voltage profile in Fig. 6b is associated with the decomposition of the SEI film, which occurs above 4.3 and 4.6 V. Thus, we state here that $Li_4Ti_5O_{12}$ can be cycled in 1.0–5.0 V with a charge capacity of 160 mAh g^{-1} or 0.0–4.0 V with a reversible capacity of 220 mAh g^{-1}. Moreover, it indicates that $Li_4Ti_5O_{12}$ still maintains its high structure stability after cycling between 1.0 and 5.0 V (Fig. 7).

Conclusions

The structure of $Li_4Ti_5O_{12}$ is maintained in a broad electrochemical window (0.0–5.0 V). $Li_4Ti_5O_{12}$ can deliver a reversible capacity of 160 mAh g^{-1} in 1.0–5.0 V and a charge capacity of 220 mAh g^{-1} in 0.0–4.0 V. In addition, superior rate behaviors are presented in the voltage range 0.0–2.0 V. A reversible specific capacity of 150 mAh g^{-1} can be achieved at a current density of 7.8 mA cm^{-2} in a voltage range from 0.0 to 2.0 V.

Acknowledgments The author truly thanks Prof. Pengfei Shi of Harbin Institute of Technology and Dr. Xuejie Huang, Dr. Hong Li, and Dr. Zhaoxiang Wang of Institute of Physics, Chinese Academy of Sciences for their helpful discussion on the experimental techniques.

References

1. Pasquier AD, Laforgue A, Simon P, Amatucci GG, Fauvarque JF (2002) J Electrochem Soc 149:A302. doi:10.1149/1.1446081
2. Abouimrane A, Lebdeh YA, Alarco PJ, Armand M (2004) J Electrochem Soc 151:A1028. doi:10.1149/1.1759971
3. Pasquier AD, Plitz I, Gural J, Badway F, Amatucci GG (2004) J Power Sources 136:160. doi:10.1016/j.jpowsour.2004.05.023
4. Panero S, Reale P, Ronci F, Scrosati B, Perfetti P, Albertini VR (2001) Phys Chem Chem Phys 3:845. doi:10.1039/b008703n
5. Kanamura K, Umegaki T, Naito H, Takehara Z, Yao T (2001) J Appl Electrochem 31:73. doi:10.1023/A:1004170009354
6. Scharner S, Weppner W, Schmid-Beurmann P (1999) J Electrochem Soc 146:857. doi:10.1149/1.1391692
7. Wang GX, Bradhurst DH, Dou SX, Liu HK (1999) J Power Sources 83:156. doi:10.1016/S0378-7753(99)00290-6
8. Ohzuku T, Ueda A, Yamamoto N (1995) J Electrochem Soc 142:1431. doi:10.1149/1.2048592
9. Nakahara N, Nakajima R, Matsushima T, Majima H (2003) J Power Sources 117:131. doi:10.1016/S0378-7753(03)00169-1
10. Ohta N, Takada K, Zhang LQ, Ma RZ, Osada M, Sasaki T (2006) Adv Mater 18:2226. doi:10.1002/adma.200502604
11. Liu DQ, Liu XQ, He ZZ (2007) Mater Chem Phys 105:362. doi:10.1016/j.matchemphys.2007.04.073
12. Shu J (2008) Electrochem Solid-State Lett 11:A238
13. Aldon L, Kubaik P, Womes M, Jumas JC, Fourcade JO, Tirado JL, Corredor JI, Vicente CP (2004) Chem Mater 16:5721. doi:10.1021/cm0488837
14. Poizot P, Laruelle S, Grugeon S, Tarascon JM (2002) J Electrochem Soc 149:A1212. doi:10.1149/1.1497981
15. Li H, Richter G, Maier J (2003) Adv Mater 15:736. doi:10.1002/adma.200304574
16. Li H, Balaya P, Maier J (2004) J Electrochem Soc 151:A1878. doi:10.1149/1.1801451
17. Balaya P, Li H, Kienle L, Maier J (2003) Adv Funct Mater 13:621. doi:10.1002/adfm.200304406
18. Laruelle S, Grugeon S, Poizot P, Dolle M, Dupont L, Tarascon JM (2002) J Electrochem Soc 149:A627. doi:10.1149/1.1467947